Rock and Soil Mechanics

Volume 43 | Issue 3 Article 3

5-17-2022

# Prediction model of saturated/unsaturated permeability coefficient of compacted loess with different dry densities

Hai-man WANG

Wan-kui NI



## Custom Citation

WANG Hai-man, NI Wan-kui. Prediction model of saturated/unsaturated permeability coefficient of compacted loess with different dry densities[J]. Rock and Soil Mechanics, 2022, 43(3): 729-736.

Rock and Soil Mechanics 2022 43(3): 729−736 ISSN 1000−7598
https: //doi.org/10.16285/j.rsm.2021.5735 rocksoilmech.researchcommons.org/journal

# Prediction model of saturated/unsaturated permeability coefficient of compacted loess with different dry densities

WANG Hai-man, NI Wan-kui
College of Geology Engineering and Geomatics, Chang'an University, Xi'an, Shaanxi 710054, China

**Abstract:** The direct measurement of unsaturated permeability coefficient is costly and the accuracy cannot be fully guaranteed. Therefore, the establishment of a simple and practical prediction model for saturated/unsaturated permeability coefficient based on Darcy's law has important theoretical and practical significance. In this paper, a self-made unsaturated permeability device was used to test the unsaturated permeability coefficient of Yan'an compacted loess with different dry densities, and the pore size distribution curve was determined by nuclear magnetic resonance technology. Based on the characteristics of pore distribution, Darcy's theorem is differentiated, and the relationship model between pore ratio and saturated/unsaturated permeability coefficient is established. The research results show that the parameters ($D$ and $B$) in the prediction model can be determined by the slope and intercept of the cumulative pore volume at two points (peak point and half-width point) on the pore size distribution curve and the pore size in a straight line in double logarithmic coordinates; the porosity ratio and the dominant pore diameter have a linear relationship in the double logarithmic coordinates, and the model parameters can be expressed by the porosity ratio; the predicted results of the model are basically consistent with the measured values, which suggests that the proposed model is simple, reliable and practical.

**Keywords:** compacted loess; unsaturated infiltration; permeability coefficient; pore size distribution; prediction model

## 1 Introduction

The land reclamation project in Yan'an New District has formed a large amount of compacted loess with varying physical properties. Different parts of the project have different compaction requirements, giving rise to loess deposits with varying degrees of compaction. The coefficient of permeability and seepage law of soil are important topics in soil mechanics and geotechnical engineering. The seepage of unsaturated soil has a significant influence on matrix suction, consolidation deformation, earth pressure, soil strength, and soil damage[1]. Therefore, studying the coefficient of permeability of the Yan'an compacted loess during compression has theoretical and practical significance.

Due to the complexity of unsaturated soils, studying the coefficient of permeability of unsaturated soils is difficult and essential. Because the direct measurement of the coefficient of permeability requires special testing equipment and is technically demanding, various models have been proposed to estimate the coefficient of permeability using the relatively easy-to-measure water holding capacity[2−7]. However, the accuracy of these models is difficult to guarantee, and the physical meaning of the resulting parameters is not clear. In addition, these models can only determine the soil coefficient of permeability in a specific state and cannot predict the coefficient of permeability of soil with different dry densities. Therefore, it is of great significance to establish a mathematical model that can accurately predict the coefficient of permeability for compacted soil with different dry densities.

The empirical prediction method is commonly used to predict the coefficient of permeability during deformation[8−9], i.e., an empirical formula is obtained using a large number of statistics. However, the pore structure of different soils can vary significantly, and the applicability of the empirical formula has great limitations. As a water flow channel, pore plays a controlling role in soil infiltration; however, the empirical method does not reveal the infiltration mechanism from the perspective of microscopic pore channels. Therefore, two main problems must be solved when predicting the coefficient of permeability during deformation: (1) The evolution of pore distribution during deformation; for example, Li et al.[10] and Wang et al.[11] assumed that the pore size distribution curve conformed to a normal distribution within a semi-logarithmic coordinate system and established the mathematical expression of the pore size distribution curve. Tao et al.[12] found that the cumulative pore size distribution curves of clayey soil specimens with different pore ratios during compression had a "broomstick" distribution by a series of means such as mercury intrusion porosimetry (MIP),

Received: 15 May 2021 Revised: 14 December 2021
This work was supported by the National Natural Science Foundation of China(41931285).
First author: WANG Haiman, male, born in 1993, PhD candidate, mainly engaged in the research of unsaturated soil mechanics of loess. E-mail: 1164727259@qq.com
Corresponding author: NI Wankui, male, born in 1965, Professor, mainly engaged in the research and teaching of loess mechanics. E-mail: niwankui@chd.edu.cn

and proposed a pore size distribution curve prediction method. (2) Establish the relationship between the pore distribution curve and the unsaturated coefficient of permeability. For example, Chen[13] and Tao et al.[14] proposed a method for predicting the unsaturated coefficient of permeability based on microscopic pore channels by combining the hydrodynamic theory. Theoretically, the unsaturated coefficient of permeability under deformation conditions can be obtained using the above two research results. However, in order to better serve engineering practice, the pore size distribution curve prediction parameters should be combined with macroscopic physical parameters to predict the pore size distribution curve without relying on modern microscopic testing methods such as MIP.

Based on the above concept, this paper proposes a prediction model for saturated/unsaturated coefficient of permeability using microscopic pores based on Darcy's law. Then the model is optimized using the pore size distribution characteristics, and a model using the relationship between void ratio and saturated/unsaturated coefficient of permeability is established.

## 2 Materials and methods

### 2.1 Materials

The loess used in this study was sampled from Yan'an New District, China. The soil at the sampling point was $Q_3$ loess. The basic physical indicators of the soil used in the test are shown in Table 1. The natural moisture content was about 26%, the optimum moisture content was 14.11%, the plastic limit $w_p$ was 16.1%, the liquid limit $w_L$ was 28.9%, and the plasticity index $I_P$ was 12.8. Heavy compaction was used in the filling of Yan'an New District. The homemade unsaturated permeameter used in the subsequent permeation test was large in size (30 cm in diameter and 60 cm in height), and the larger compaction energy would cause the side walls of the glass drum to be damaged by excessive forces, making it difficult to prepare specimens with larger dry densities. In addition, the main objective of this paper is to present a saturated/unsaturated permeability model based on the void ratio, and therefore, it is applicable to any dry density soil (including heavy compaction specimens) in a strict sense. Thus, the compaction tests in this paper used light compaction with a maximum dry density of 1.69 g /cm$^3$. The particle size distribution was analyzed using a Bettersize2000 laser particle size analyzer, and the results indicated that loess samples were predominantly composed of silt (about 78.99%), with approximately the same sand and clay content of 10.39% and 10.62%, respectively (Fig.1).

**Table 1 Basic physical parameters of soil samples**

| Property | Maximum dry density $\rho_d$ /(g • cm$^{-3}$) | Optimal water content $w$ /% | Specific gravity $G_s$ | Liquid limit $w_L$ /% | Plastic limit $w_P$ /% | Particle size distribution /% | | |
|---|---|---|---|---|---|---|---|---|
| | | | | | | Sand | Silt | Clay |
| Value | 1.69 | 14.11 | 2.72 | 28.9 | 16.1 | 10.39 | 78.99 | 10.62 |

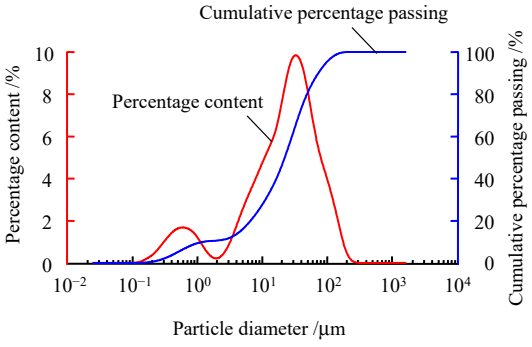


**Fig. 1 Soil particle size distribution curves**

### 2.2 Method

The loess samples were crushed using a rubber mallet and air-dried and passed through a 2 mm sieve to configure loose soil with a moisture content of 10%. The loose soil was placed in an incubator to allow sufficient moisture uniformity for sample preparation.

#### 2.2.1 Saturated permeability test

The above-mentioned loose soil was compacted into a sample with a height of 40 mm, a diameter of 61.8 mm, and dry densities of 1.45, 1.55, and 1.65 mg /m$^3$. Two samples were prepared for each dry density, totaling 6 samples. In order to eliminate accidental errors, if the test results for two samples with the same dry density differed by more than 5%, the third sample was selected for testing until the test results of the same dry density samples differed by less than 5%. The saturated coefficient of permeability was tested by the variable head method at 20±2 ℃, using the TST-55 permeability meter produced by the Nanjing Soil Instrument Factory.

#### 2.2.2 Unsaturated permeability test

This paper adopted the instantaneous profile method and a self-made plexiglass barrel to measure the unsaturated coefficient of permeability (Fig.2). The specific parameters

and dimensions of the device are given in the reference[15]. A small hole with a diameter of 0.8 cm was evenly distributed every 10 cm on both sides of the plexiglass barrel. The MPS-6 water potential sensor and EC-5 moisture sensor were buried in small holes at each height for water potential and moisture testing. The prepared loose soil with a moisture content of 10% was layered and compacted within the barrel to the target dry density. The target dry densities were 1.45, 1.55, and 1.65 Mg /m$^3$, each layer was 5 cm high for a total of 10 layers, and the soil interface was shaved. A set of sensors was set every 10 cm, with four sets in total. A 10 cm thick glass bead was placed on the upper part of the soil column to prevent compaction of the soil surface or water seepage along the sidewall during the simulated rainfall process. A water spray can be used to simulate rainfall, and the total spraying time was 30 minutes with a rainfall volume of 4 400 mL. Immediately after the rainfall ended, the top of the soil column was sealed with plastic wrap to prevent water from evaporating. The entire moisture infiltration process could be clearly observed through the transparent plexiglass barrel. Meanwhile, the sensors recorded water potential and moisture data in real time.

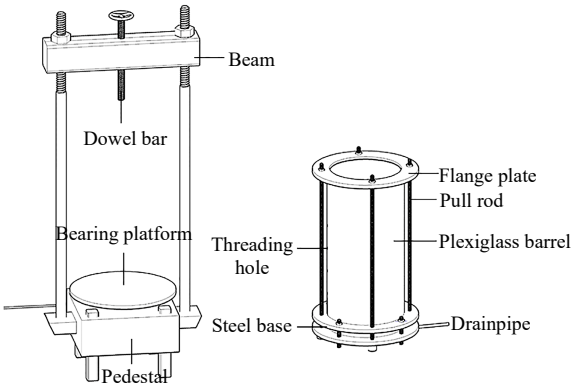


**Fig. 2 Schematic diagram of unsaturated permeameter**

## 3 Saturated/unsaturated coefficient of permeability prediction model

### 3.1 Model building

In a steady flow state, Darcy's theorem is also applicable to unsaturated infiltration[16], and from Darcy's theorem it follows that:

$$K = \frac{Q}{Ai} \tag{1}$$

where $K$ is the coefficient of permeability; $A$ is the sectional area of the sample; $Q$ is the sample volume flow rate; and $i$ is the hydraulic gradient.

Due to the existence of a huge amount of connected pores in the soil, seepage occurs in these connected pores. In addition, unsaturated soil always fills smaller pores size during humidification. As the matrix suction attenuate, water gradually moves into the macropores. Thus the idea of integration can be used to divide the pores into $n$ grades based on the pore size (Fig.3). Therefore, the pore flow $Q$ of the sample can be expressed as the sum of the pore volume flow of the first $m$ grades ($m \leqslant n$):

$$Q = \sum_{j=1}^{m} q_j \tag{2}$$

where $q_j$ is the volume flow of the $j$-th grade pore.

According to the Hagen Poiseuille formula, the volume flow $q_j$ in the pore of the grade $j$ can be expressed as

$$q_j = \frac{\pi r_j^4 \cdot \Delta p}{8\eta l} \tag{3}$$

where $r_j$ is the pore radius; $\Delta p$ is the pressure difference between the two ends of the pore; $\eta$ is the viscosity coefficient; and $l$ is the pore length. Assuming that the ratio of pore length ($l$) to sample length ($L$) is $p_j$, the pore length can be expressed as $Lp_j$.

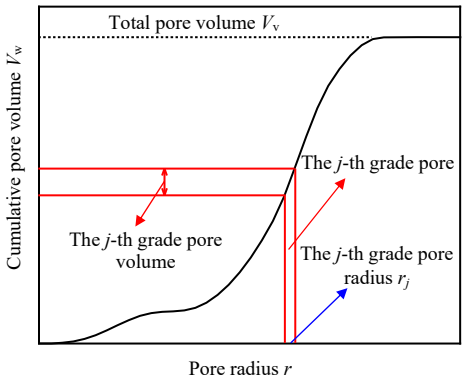


**Fig. 3 Diagram of aperture classification**

According to the fractal model theory of pore volume distribution, the relationship between pore radius and the corresponding number is[17]:

$$N = Cr^{-D} \tag{4}$$

where $C$ is a constant; $D$ is the fractal dimension of pore distribution; and $N$ is the number of pores.

Therefore, Eq.(1) can be expressed as

$$K = \frac{\sum_{j=1}^{m} \frac{\pi r_j^4 \cdot \Delta p}{8\eta L p_j} N}{Ai} \tag{5}$$

Due to the $j$-th grade pore cross-sectional area $A_j = \pi r_j^2$, the water head loss $\Delta h = \frac{\Delta p}{\rho g}$, and the hydraulic

gradient $i=\dfrac{\Delta h}{L}$, therefore, Eq.(5) can be wrritten as

$$K=\frac{\rho g}{8\eta A}\sum_{j=1}^{m}\frac{r_j^2 A_j}{p_j}N \tag{6}$$

where $\rho$ is the density of water (g /cm$^3$); and $g$ is the acceleration of gravity.

The volume of liquid in the $j$-th pore is $\Delta V_{\mathrm{w}}$, so $A_i N=\dfrac{\Delta V_{\mathrm{w}}}{Lp_j}$; therefore, Eq.(6) can be further expressed as

$$K=\frac{\rho g}{8\eta V}\sum_{j=1}^{m}\frac{r_j^2\cdot\Delta V_{\mathrm{w}}}{p_j^2} \tag{7}$$

where $V$ is the sample volume.

Tao and Kong[14] suggested that for an ideal hypothesis model $p_j$ is a constant, so the above formula can be abbreviated as

$$K=\frac{K_{\mathrm{c}}}{V}\sum_{j=1}^{m}r_j^2\cdot\Delta V_{\mathrm{w}} \tag{8}$$

where $K_{\mathrm{c}}=\dfrac{\rho g}{8\eta p_j^2}$. For the same soil $K_{\mathrm{c}}$ is a constant.

From Eq.(4), the pore volume $V_{\mathrm{w}}$ with pore radius less than $r$ can be expressed as

$$V_{\mathrm{w}}=\int_0^r\left(\frac{4\pi r^3}{3}\right)\mathrm{d}N=Br^{3-D} \tag{9}$$

where $B=4\pi CD(D-3)/3$.

Therefore, Eq.(8) can be written in integral form:

$$K=\frac{K_{\mathrm{c}}}{V}\int_0^{V_{\mathrm{w}}}\left(\frac{V}{B}\right)^{\frac{2}{3-D}}\mathrm{d}V=\frac{(3-D)K_{\mathrm{c}}}{(5-D)V}\left(\frac{1}{B}\right)^{\frac{2}{3-D}}V_{\mathrm{w}}^{\frac{5-D}{3-D}} \tag{10}$$

Equation (10) is the coefficient of permeability when the liquid phase volume in the soil is $V_{\mathrm{w}}$. When the pores in the soil are completely filled with liquid ($V_{\mathrm{w}}=V_{\mathrm{v}}$), the coefficient of permeability is the saturated coefficient of permeability $K_{\mathrm{s}}$. The unsaturated relative coefficient of permeability $K_{\mathrm{r}}$ can also be expressed as

$$K_{\mathrm{r}}=\frac{K}{K_{\mathrm{s}}}=(S_{\mathrm{r}})^{\frac{5-D}{3-D}} \tag{11}$$

where $S_{\mathrm{r}}$ is the degree of saturation. Eq.(11) is similar to the Campbell-Norman model in form, and both are exponential of the degree of saturation, which proves the rationality of the model from the side.

### 3.2 Parameter solution

According to the NMR results, soil with unit mass (1 g) particles was analyzed (Fig.4). The cumulative pore size distribution curve can be obviously divided into three stages. Because of the large distribution range and small distribution quantity of macropores in soil, macropores do not conform to fractal geometry characteristics. Generally, pores with a diameter greater than 32 μm are considered to be macropores[18]; therefore, the boundary between the second and third stages is 32 μm. The third stage data is discarded when calculating the fractal dimension. For smaller pores, the water in the pore is generally considered to exist in the form of bound water, which is not suitable for the capillary theory; therefore, this data should also be excluded[19]. The half amplitude point method is generally used to determine the amount of bound water. The pore diameter at 1/2 of the highest point of the pore size distribution curve is taken as the critical pore diameter[20]. The critical pore size $d_{\mathrm{r}}$ of the samples with different dry densities was all 3.8 μm, and the bound water content was 52.76 mm$^3$ /g (Fig.4). Since pores with a diameter of less than 3.8 μm are not suitable for pore fractal theory, the boundary between the first stage and the second stage is 3.8 μm, and the first stage data is discarded when calculating fractal dimension.

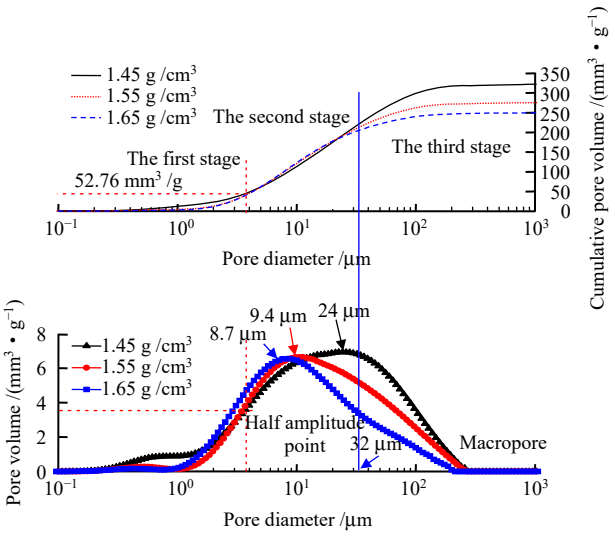


**Fig. 4 Pore size distribution curves**

The logarithm of both sides of Eq.(9) is

$$\lg V_{\mathrm{w}}=(3-D)\lg r+\lg B \tag{12}$$

Since the pore diameter $d$ is twice the radius $r$ ($d=2r$), Eq.(12) can be expressed again as

$$\lg V_{\mathrm{w}}=(3-D)\lg d+\lg\frac{B}{2^{3-D}} \tag{13}$$

From Eq.(13), if the pore volume and the pore diameter

are the logarithms of base 10, and the slope of the scatter plot is $k$, then $D = 3-k$ can be made, the intercept is $b$, and then $B = 10^b \cdot 2^k$.

The data that fit the fractal model (the second stage data) were sorted, and a scatter plot was plotted with lg$d$ as the abscissa and lg$V_w$ as the ordinate (Fig.5). The data exhibited an apparent linear relationship, and these data were linearly fitted to $y = kx + b$. The fitted expression and parameters are shown in Table 2, where $R^2$ is the coefficient of determination.

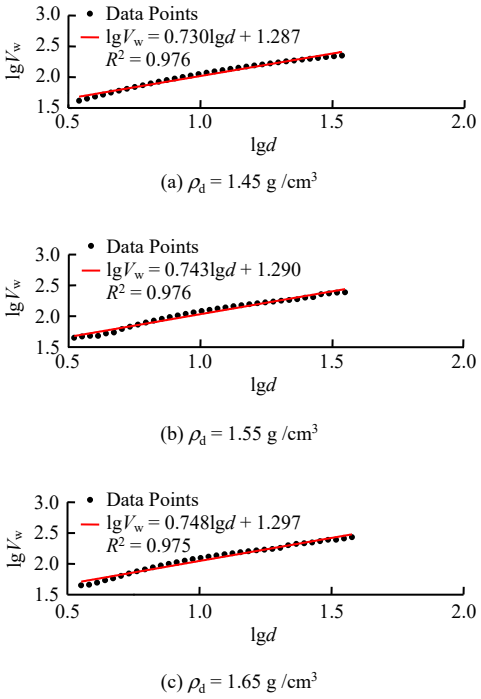


**Fig. 5 Calculation of fractal dimension**

**Table 2 Linear fitting results**

| Dry density /(g • cm$^{-3}$) | $k$ | $b$ | $R^2$ | $D$ | $B$ |
|---|---|---|---|---|---|
| 1.45 | 0.730 | 1.287 | 0.976 | 2.270 | 32.12 |
| 1.55 | 0.740 | 1.290 | 0.976 | 2.266 | 32.43 |
| 1.65 | 0.748 | 1.297 | 0.975 | 2.252 | 33.28 |

It can be seen from Table 2 that the coefficients of determination of samples of different dry densities were all greater than 0.97, indicating that the fitting effect was good. At this time, the fractal dimension $D$ and parameter $B$ of the different dry density samples have been calculated. $K_c$ is a constant for the same soil type, so the saturated/unsaturated coefficient of permeability of samples with arbitrary dry densities can be predicted on the basis of the known pore diameter distribution curves.

### 3.3 Model optimization

Although the above model can predict the saturated and unsaturated coefficient of permeability of samples with different dry densities, measuring the pore size distribution curve of each sample is difficult to achieve in practical applications and can not be realized in real time during the compression process. Therefore, the above model should be optimized.

As the dry density of the sample increased, the dominant pore diameter $d_a$ moved to the left, that is, $d_a$ decreased as the void ratio $e$ decreased. For example, if the dry density of the sample increased from 1.45 g /cm$^3$ to 1.65 g /cm$^3$, $d_a$ was reduced from 24 μm to 8.7 μm (Fig.4). The relationship curve between $e$ and $d_a$ was plotted in logarithmic coordinates (Fig.6). It was obvious that $e$ and $d_a$ had a linear relationship. Phadnis and Santamarina[21] also found the same pattern, and deduced from the theoretical level that $e$ and $d_a$ had a linear relationship. Comparing with the results of Wang et al.[11] (Fig.6), it was found that the slope of the linear relationship between $e$ and $d_a$ was basically the same, except for the intercept, which might vary from soil to soil.

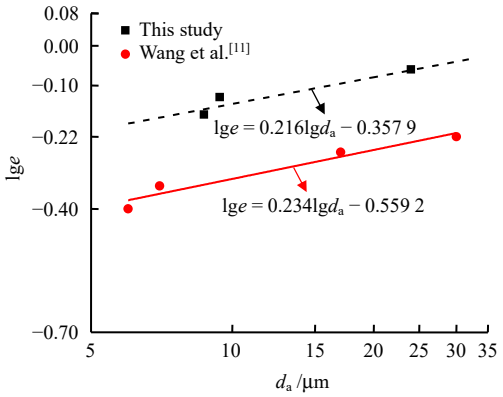


**Fig. 6 Relationship between $e$ and $d_a$**

Li et al.[10] assumed that the pore size distribution curve conformed to a normal distribution in a semi-logarithmic coordinate system, and the shape of the pore size distribution curve did not change significantly during compression. According to properties of the normal distribution, the cumulative pore volume of pores with a diameter less than the dominant pore diameter $d_a$ is $e/(2G_s)$. Combining the results of Fig.5 and the characteristics of normal distribution, the dominant pore size and the corresponding cumulative pore volume can be calculated when the pore ratio $e$ is known. Li et al.[22] and Liu et al.[23] proposed that the volume of tiny pores hardly changed with the change of dry density, which was consistent with the results of this study (Fig.4). In other words, the volume of pores smaller than 3.8 μm did not change with varying dry density. The pore volume with a pore diameter of less than 3.8 μm is calculated to

be 52.76 mm$^3$ /g. According to the above two points (peak point and half amplitude point), a straight line of $d$ and $V_w$ similar to Fig.5 can be determined in double logarithmic coordinates. The slope $k$ and intercept $b$ are

$$k=\frac{\lg\frac{e}{2G_s}-\lg 52.76}{\lg d_a-\lg 3.8} \tag{14}$$

$$b=\lg 52.76-k\lg 3.8 \tag{15}$$

As can be seen from Fig.6 that $\lg d_a=(\lg e+0.357\,9)/0.216$, so the slope $k$ can be expressed as

$$k=0.216\frac{\lg\frac{e}{2G_s}-\lg 52.76}{\lg e+0.357\,9-0.216\cdot\lg 3.8} \tag{16}$$

Then the fractal dimension $D$ can be expressed as

$$D=3-0.216\frac{\lg\frac{e}{2G_s}-\lg 52.76}{\lg e+0.357\,9-0.216\cdot\lg 3.8} \tag{17}$$

From Eqs.(13) and (15), $B$ is:

$$B=52.76\cdot 0.526^k \tag{18}$$

For the same kind of soil, the parameters $D$ and $B$ are only related to the void ratio, and measuring the pore size distribution curve is not necessary in the model, which can effectively reduce the difficulty of parameter calculation.

## 4 Model validation

Section 3.1 presents the saturated/saturated coefficient of permeability prediction model, and Section 3.3 provides a convenient way to obtain unknown parameters. Since all these parameters are related to the void ratio, water content and saturated coefficient of permeability only, it is possible to calculate the saturated/unsaturated coefficient of permeability during the compaction of compacted loess.

### 4.1 Validation of saturated coefficient of permeability prediction model

Using the saturated permeability test, the saturated coefficient of permeabilitys of samples with different dry densities can be obtained (Table 3). Taking the 1.45 g /cm$^3$ dry density sample as an example, when the void ratio $e$ is known, the parameters $D$ and $B$ can be obtained by applying Eqs.(17) and (18), respectively. Using a soil sample containing a unit mass (1 g) as the object of study, the soil volume $V$ and pore volume $V_v$ are $(1+e)/G_s$ and $e/G_s$, respectively. At this time, the constant $K_c$ can be obtained by using the saturated coefficient of permeability of the 1.45 g /cm$^3$ dry density sample obtained from the test. The above steps are repeated when predicting the saturated coefficients of permeability of samples with different void ratios. Since $K_c$ is a constant, which has been obtained from the dry density sample of 1.45 g /cm$^3$, the saturated coefficient of permeability of the sample with different dry densities can be obtained by using Eq.(10) (Table 3). It can be seen that although there is a certain deviation between the predicted value and the test value, the two are of the same order of magnitude, indicating that the model proposed in this paper can be used to predict the saturated coefficient of permeability of Yan'an compacted loess.

**Table 3 Tested value and predicted value of saturated coefficient of permeability**

| $\rho_d$ /(g • cm$^{-3}$) | Tested $K_s$ /(cm • s$^{-1}$) | Predicted $K_s$ /(cm • s$^{-1}$) |
|---|---|---|
| 1.45 | $1.18\times10^{-4}$ | — |
| 1.55 | $6.14\times10^{-5}$ | $2.83\times10^{-5}$ |
| 1.65 | $2.35\times10^{-5}$ | $1.18\times10^{-5}$ |

The parameters $D$ and $B$ calculated according to Eqs.(17) and (18) in Table 4 are consistent with the measured results in Table 2, indicating that the optimized model can determine the parameters easily, and the results have certain reliability.

**Table 4 Parameters needed for permeability coefficient prediction**

| $\rho_d$ /(g • cm$^{-3}$) | $e$ | $D$ | $B$ | $V$ /(mm$^3$ • g$^{-1}$) | $V_v$ /(mm$^3$ • g$^{-1}$) | $K_c$ |
|---|---|---|---|---|---|---|
| 1.45 | 0.87 | 2.39 | 36.94 | 689.66 | 320.65 | $8.84\times10^{-7}$ |
| 1.55 | 0.75 | 2.25 | 34.07 | 645.16 | 276.16 | $8.84\times10^{-7}$ |
| 1.65 | 0.64 | 2.12 | 30.07 | 606.06 | 237.06 | $8.84\times10^{-7}$ |

### 4.2 Validation of unsaturated coefficient of permeability prediction model

During infiltration, the total head $h_w$ at any position $z_j$ without considering the osmotic pressure head is equal to the sum of the position head $z_j$ and the matrix suction head $h_m$, that is

$$h_w=z_j+h_m \tag{19}$$

The hydraulic gradient $i_w$ at point $z_j$ at time $t$ is equal to the slope of the head distribution line at that point, that is

$$i_w=\frac{h_w}{\mathrm{d}z} \tag{20}$$

The water volume $V_w$ between point $z_j$ and the top of the soil column is

$$V_{\mathrm{w}}=\int_0^{z_j}\theta_{\mathrm{w}}(z)_t A\mathrm{d}z \tag{21}$$

where $A$ is the cross-sectional area of the soil column (cm$^2$); and $\theta_{\mathrm{w}}(z)_t$ is the volumetric water content at point $z$ at time $t$.

The flow velocity $v_{\mathrm{w}}$ at point $z_j$ can be expressed as

$$v_{\mathrm{w}}=\frac{\mathrm{d}V_{\mathrm{w}}}{A\,\mathrm{d}t} \tag{22}$$

The unsaturated coefficient of permeability $k_{\mathrm{w}}$ is

$$k_{\mathrm{w}}=-\frac{v_{\mathrm{w}}}{i_{\mathrm{ave}}} \tag{23}$$

where $i_{\mathrm{ave}}$ is the average hydraulic gradient of the point within the selected time.

The forward difference method is used when calculating $i_{\mathrm{ave}}$, that is

$$i_{\mathrm{ave}}=\frac{1}{2}\left(\frac{h_{\mathrm{w}(j+1),t_1}-h_{\mathrm{w}(j),t_1}}{z_{j+1}-z_j}+\frac{h_{\mathrm{w}(j+1),t_2}-h_{\mathrm{w}(j),t_2}}{z_{j+1}-z_j}\right) \tag{24}$$

where $h_{\mathrm{w}(j),t}$ is the water head at point $z_j$ at time $t$.

According to the volumetric water content and matrix suction monitored by the water potential sensor and the moisture sensor, the relationship between the unsaturated coefficient of permeability and volumetric water content of compacted loess with different dry densities can be calculated using the instantaneous profile method (Fig.7).

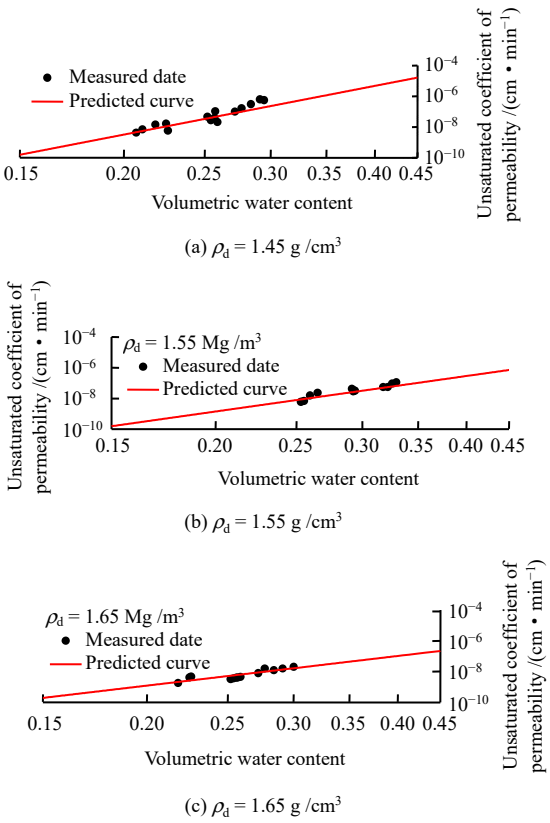


(a) $\rho_{\mathrm{d}}$ = 1.45 g /cm$^3$

(b) $\rho_{\mathrm{d}}$ = 1.55 g /cm$^3$

(c) $\rho_{\mathrm{d}}$ = 1.65 g /cm$^3$

**Fig. 7 Measured unsaturated coefficient of permeability and predicted curve**

The method for solving the parameters of the unsaturated permeability prediction model is the same as the method for solving the parameters of the saturated coefficient of permeability. The predicted relationship curve between the unsaturated coefficient of permeability and the volumetric water content of the three dry density samples can be obtained by substituting the parameters in Table 4 into Eq.(10) (Fig.7).

Figure 7 inidcates that the measured and predicted values of the unsaturated coefficient of permeability are in general agreement. It shows that it is feasible to predict the saturated/unsaturated coefficients of permeability of arbitrary void ratio samples according to the above method for Yan'an compacted loess where the void ratio and saturated coefficient of permeability are known in a certain state.

In summary, the prediction model proposed in this paper is simple, reliable and practical, and can provide technical support for the study of unsaturated soil seepage during deformation.

## 5 Conclusions

The relationship model between the void ratio and saturated/unsaturated coefficient of permeability of Yan'an compacted loess was established, and the accuracy of the model was verified. The following conclusions can be drawn:

(1) Darcy's theorem is still applicable to unsaturated seepage flow, and the saturated/unsaturated coefficient of permeability can be derived by differentiating Darcy's theorem based on the microscopic pore distribution characteristics.

(2) The important parameters (fractal dimension $D$ and parameter $B$) in the saturated/unsaturated coefficient of permeability expression can be determined by the slope and intercept of a straight line formed in double logarithmic coordinates between the cumulative pore volume and the pore size. When calculating the fractal dimension of Yan'an compacted loess, the pore size distribution data between 3.8 and 32.0 μm should be used for calculation.

(3) The void ratio and dominant pore size have a linear relationship in double logarithmic coordinates, and the slope of the soil in different regions is essentially the same, but the intercept is different. Both the fractal dimension $D$ and the parameter $B$ can be expressed in terms of the void ratio.

(4) The calculated results of the void ratio-based coefficient of permeability prediction model and the measured

data are generally consistent, indicating that the saturated/ unsaturated coefficient of permeability prediction model proposed in this paper is reliable for the coefficient of permeability prediction of the Yan'an compacted loess.

## References

[1] LIU Zu-dian. Loess mechanics and engineering[M]. Xi'an: Shaanxi Science and Technology Press, 1997.

[2] HUNT A, GHANBARIAN B, SAVILLE K. Unsaturated hydraulic conductivity modeling for porous media with two fractal regimes[J]. Geoderma, 2013, 207: 268−278.

[3] LEBEAU M, KONRAD J. A new capillary and thin film flow model for predicting the hydraulic conductivity of unsaturated porous media[J]. Water Resources Research, 2010, 46(12): W12554.

[4] GUI M, HSU C. Generalized fitting parameters of three permeability functions for predicting water coefficient of permeability of lateritic soil[J]. Geotechnical Testing Journal, 2009, 32(5): J101910−J101931.

[5] FREDLUND D G, XING A. Equations for the soil-water characteristic curve[J]. Canadian Geotechnical Journal, 1994, 31(6): 1023−1025.

[6] GARDNER W R. Mathematics of isothermal water conduction in unsaturated soil[J]. Highway Research Board Special Report, 1958, 40: 78−87.

[7] GENUCHTEN V T M. A closed-form equation for predicting the hydraulic conductivity of unsaturated soils[J]. Soil Science Society of America Journal, 1980, 44(5): 892−898.

[8] REICOSKY D C, VOORHEES W B, RADKE J K. Unsaturated water flow through a simulated wheel track[J]. Soil Science Society of America Journal, 1981, 45(1): 3−8.

[9] DENG Yong-feng, LIU Song-yu, ZHANG Ding-wen, et al. Comparison among some relationships between permeability and void ratio[J]. Northwestern Seismological Journal, 2011, 33(Suppl.1): 64−66.

[10] LI P, SHAO S, VANAPALLI S. Characterizing and modeling the pore-size distribution evolution of a compacted loess during consolidation and shearing[J]. Journal of Soils and Sediments, 2020, 20(7): 2855−2867.

[11] WANG J, LI P, MA Y, et al. Evolution of pore-size distribution of intact loess and remolded loess due to consolidation[J]. Journal of Soils and Sediments, 2019, 19(3): 1226−1238.

[12] TAO Gao-liang, ZHANG Ji-ru, ZHUANG Xin-shan, et al. Influence of compression deformation on the soil-water characteristic curve and its simplified representation method[J]. Journal of Hydraulic Engineering, 2014, 45(10): 1239−1246.

[13] CHEN Yin. Prediction approach of permeability coefficient of unsaturated soil based on nuclear magnetic resonance technique[D]. Wuhan: Hubei University of technology, 2019.

[14] TAO Gao-liang, KONG Ling-wei. A model for determining the permeability coefficient of saturated and unsaturated soils based on micro pore channel and its application[J]. Journal of Hydraulic Engineering, 2017, 48(6): 702−709.

[15] ZHANG Zhen-fei, NI Wan-kui, WANG Xi-jun, et al. An experimental study of water infiltration and hydraulic-conductivity of the compacted loess[J]. Hydrogeology and Engineering Geology, 2019, 46(6): 97−104.

[16] TIAN K, YANG A, NIE K, et al. Experimental study of steady seepage in unsaturated loess soil[J]. Acta Geotechnica, 2020, 15(9): 2681−2689.

[17] PFEIFER P, AVNIR D. Chemistry in noninteger dimensions between two and three. I. Fractal theory of heterogeneous surfaces[J]. Journal of Chemical Physics, 1983, 79(7): 3558−3565.

[18] LEI Xiang-yi. Pore types and collapsibility of loess in China[J]. Scientia Sinical (Chemical), 1987(12): 1309−1318.

[19] TAO Gao-liang, CHEN Yin, YUAN Bo, et al. Predicting soil-water retention curve based on NMR technology and fractal theory[J]. Chinese Journal of Geotechnical Engineering, 2018, 40(8): 1466−1472.

[20] ZHANG Shi-min, SUN Yin-suo, ZHANG Li-sha, et al. Application of nuclear magnetic resonance technology in pore analysis of unfrozen soil[J]. Yangtze River, 2019, 50(11): 183−188.

[21] PHADNIS H S, SANTAMARINA J C. Bacteria in sediments: pore size effects[J]. Géotechnique Letters, 2015, 1(4): 91−93.

[22] LI Hua, LI Tong-lu, ZHANG Ya-guo, et al. Relationship between unsaturated permeability curve and pore-size distribution of compacted loess with different dry density[J]. Journal of Hydraulic Engineering, 2020, 51(8): 979−986.

[23] LIU De-ren, XU Shuo-chang, XIAO Yang, et al. Experimental study on the law of water-air migration in compacted loess under the condition of immersion infiltration[J]. Rock and Soil Mechanics, 2021, 42(12): 3260−3270.